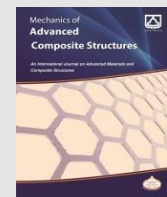




Semnan University

Mechanics of Advanced Composite Structures

Journal homepage: <https://macs.semnan.ac.ir/>ISSN: [2423-7043](#)

Research Article

Statistical Analysis of Delamination Effect on Natural Frequency of Composite Laminated Plate

Seyed Hossein Taghavian, Ahmad Reza Ghasemi *

Department of Solid Mechanics, Faculty of Mechanical Engineering, University of Kashan, Kashan 87317-51167, Iran

ARTICLE INFO

ABSTRACT

Article history:

Received: 2024-12-07

Revised: 2025-03-16

Accepted: 2025-04-16

Keywords:

Laminated plate;
Vibration characteristics;
Delaminated regions;
High-Risk zone ratio;
Frequency shift;

This study examines the free vibration behavior of composite laminated plates featuring various delaminated regions and stacking sequences. Utilizing the first-order shear deformation theory (FSDT) in combination with the finite element method, the natural frequencies of these plates are analyzed. Specifically, the investigation considers laminated plates with different numbers, sizes, and geometric arrangements of delaminated regions across several stacking sequences. The numerical results reveal notable trends in how natural frequencies vary and how delamination size affects them, highlighting a strong dependence on the stacking sequence of the layers. Furthermore, the findings demonstrate that the impact of multiple delaminated regions on the natural frequencies is less significant than the cumulative effect of these delaminations concentrated in a single location, with this discrepancy influenced by the frequency order and stacking configurations.

© 2025 The Author(s). Mechanics of Advanced Composite Structures published by Semnan University Press.

This is an open access article under the CC-BY 4.0 license. (<https://creativecommons.org/licenses/by/4.0/>)

1. Introduction

Among the structural elements, continuous fiber-reinforced laminates are the most widely used in several engineering fields including aerospace engineering, automotive industry, sports equipment, military weapons, etc. Thus, evaluation of the defect/ imperfection effects on the mechanical properties of composite laminated plates is essential for the application and structural health monitoring (SHM) of the structures containing these structural elements. The delamination of the laminates that can occur during the manufacturing process or service life may cause a catastrophic failure in the structures. According to the structural specification of the laminates, a difference in mechanical behavior between adjacent layers results in severe stress concentrations near the delaminated region.

Also, the existence of any effective delamination causes the stiffness reduction of the structures which affects their dynamic characteristic.

There are many theories and approaches have been developed for modeling and analyzing the delamination in composite structures during the past few decades [1-4]. In this regard, many studies have been done on the free-vibration behavior of composite laminated beams and plates [5-8]. However, many studies have focused on the improvement of prior theories or presented new theories. Among these numerous studies, Reddy et al. [9-10] extended the layer-wise laminate theory to analyze the multiple delamination effect. They modeled the delamination by jump discontinuity conditions at the interfaces. Also, the strain energy release rate distribution along the boundary of delaminations was computed by a different algorithm in their

* Corresponding author.

E-mail address: ghasemi@kashanu.ac.ir

Cite this article as:

Taghavian, S.H. and Ghasemi, A. R., 2026. Statistical Analysis of Delamination Effect on Natural Frequency of Composite Laminated Plate. *Mechanics of Advanced Composite Structures*, 13(1), pp. 129-142.

<https://doi.org/10.22075/MACS.2025.36174.1776>

work. Ju et al. [11] suggested a finite element formulation for the modal analysis of the laminated plates with multiple delaminations. Their method analyses the effect of transverse shear deformations and the bending-extension coupling caused by the presence of delaminations and can be easily used to compute the natural frequencies and mode shapes of delaminated plates with any boundary conditions. A generalized layerwise finite element model was developed to analyze the delaminated region in the presented study by Kim et al [12]. They investigated the effect of multiple delaminations on the natural frequencies of laminated plates with symmetric stacking sequences in terms of number, placement, and mode shapes. The variation of curvature of vibration mode caused by delamination has been studied in detail in the work of Hu et al. [13]. Yam et al. [14] analyzed natural frequency, modal displacement, and modal strain for laminated plates with different dimensions of delamination. They found that delamination-induced change of deformation is more sensitive than that of frequency, and changes of both displacement and strain are mode-dependent. Kou [15] investigated the effect of delamination on natural frequencies of simply supported rectangular cross-ply and angle-ply laminates using the finite strip method. Hammami et al. [16] investigated the effect of increasing delamination length on the linear and nonlinear behavior of glass fiber-reinforced plastics. They presented that the natural frequencies decrease with the debonding length according to the linear vibration analysis. Also, they indicated the resonance frequency shift with increasing excitation amplitude based on nonlinear vibration analysis. In the experimental work of Khazaee et al. [17] a comprehensive investigation has been stated for the analysis of delamination effects on modal parameters of carbon fiber reinforced polymers (CFRP). They tried to justify their results using damping mechanisms of composite materials. They also claimed that their approach was able to detect damage in carbon composite laminates as small as 5% of delamination area. He et al. [18] investigate the effect of contact properties of delamination regions on the modal parameters of the composite laminated plate. Also, they analyzed the contact damping using a viscoelastic Coulomb friction model. The free vibration and impact response of laminated plates with interfacial delamination were considered by Yang et al. [19]. Their results indicate that delamination reduces the natural frequencies and the middle plane delamination possesses the largest damage effect. In the work of Kumar et al. [20] the modal analysis of delaminated composite shell structures with double curvature

geometry was considered. They observed that the effect of delamination on shell structure is more predominant in comparison with respect to the plate structures. Day et al. [21] used a finite element method to determine the effects of location of delamination on free vibration characteristics of graphite-epoxy cross-ply composite pre-twisted shallow conical shells. Menezes et al. [22] worked on a new numerical-experimental methodology to indicate the effect of design parameter variations on the dynamic response of filament wound cylinders.

A considerable amount of analytical models and numerical analyses have been stated for the localization of delamination. In fact, one of the main results of the SHM is indicating the delamination size, location, and configuration in the structures. As one of the latest researchers, He et al. [23] carried out the detection of delamination properties in two steps. The first step was based on the global damage index, which is the changes in multiple modes of frequencies. In the second step, the changes have been considered based on the wavelength of multiple fiber Bragg grating sensors as the local damage index. Joy et al. [24] analyzed the absolute errors of different surrogate modeling techniques. They also used the standard deviation of predictions made by the surrogate model to quantify the areas of uncertainty in the design space. The study of Lim et al. [25] presents an alternative strategy for the simultaneous predictions of location parameters of delamination in laminated plates grounded on the combination of random forests (RF) and natural frequency-shift damage assessment methods. Tong et al. [26] believe that most studies have received scarce attention to the prediction of delamination interface. They built individual surrogate models to indicate this parameter. Maurya et al. [27] used an artificial neural network (ANN) to determine delamination defects in carbon fiber-reinforced polymer composite. They claimed that the ANN can predict the delamination length and location in the composite laminated plate. Zhang et al. [28] proposed a new surrogate-assisted optimization (SAO) method for predicting the location and size of delaminations in laminated plates using natural frequency shifts. In the study of Sha et al. [29] delamination-induced relative natural frequency change curves in laminated composite beams have been analyzed. A novel delamination indicator was developed based on mode shape and the results of their analysis. Genetic algorithms are another approach that is considered by researchers for delamination detection in laminates [30-32]. Nag et al. [33] derived a genetic algorithm for damage identification. The combination of their algorithm

and finite element model led to accepted results in the prediction of delamination using frequency changes. Krawczuk et al. [34] analyzed genetic algorithms in the delamination identification process by setting nature frequencies as damage indicators. The optimization goal was to maximize the value of the assurance criterion of damage location in their work.

Recent studies have delved into the vibrational analysis of delaminated composite laminated plates, focusing on how delamination affects their natural frequencies. Xia et al. [35] employed a finite element model incorporating a cohesive zone to simulate delamination, finding that increased delamination size and proximity to the plate's center significantly decrease natural frequencies, with mode shapes showing notable changes in delaminated regions. Krawczuk, Ostachowicz, and Żak [36] developed a finite element model for delaminated composite beams, demonstrating that both the length and position of delamination substantially alter natural frequencies, emphasizing the importance of accurate delamination modeling in predicting vibrational behavior.

This manuscript attempts to find criteria for the assessment of the laminated plates containing internal delaminated regions using a comparison of their vibration behavior based on structural parameters and delamination geometry. In general, there is a lack of both numerical and experimental investigations on delaminated regions with different numbers and arrangements in laminated composites with different stacking sequences. This study has attempted to understand how multiple delaminated regions, compared to a single delaminated region with an equivalent total area, influence the vibrational properties of the plate. The results can help to produce a criterion for non-destructive inspection (NDI) of laminated structures.

2. FEM Implementation (Theory)

As shown in Fig. 1 a delaminated composite plate is considered where the delaminated region is located at the mid-plane of the plate. The numerical analyses are performed using ABAQUS software. According to the laminated plate specification, a full 3-D geometry is modeled using the continuum shell element known as SC8R. Also, in this model, all edges of the plate have simply supported conditions.

The SC8R element in ABAQUS software is a reduced-integration shell element specifically designed for modeling multilayered structures and shell configurations. It is particularly suitable for analyzing composite materials and multilayered plates. SC8R is an eight-node quadrilateral shell element where each node has

six degrees of freedom (three translational and three rotational). This element is commonly used in structural analyses such as composite layup studies, dynamic and static evaluations, and stability or buckling assessments.

SC8R uses reduced integration to lower computational costs and prevent shear locking, a common issue in thin-shell modeling. This technique employs a single integration point at the center of the element, enhancing computational efficiency. The element supports the modeling of laminated plates with different layer properties, such as thickness, fiber orientation, and material characteristics. It is particularly effective for accurately determining the stress and strain distributions across the layers of a composite structure. The element relies on classical laminated plate theory (CLPT) and first-order shear deformation theory (FSDT) to account for the mechanical behavior of laminated shells, including shear deformation effects.

The SC8R element assumes a linear variation of strain through the thickness and incorporates shear deformation for more accurate results in moderately thick shells. It uses reduced-integration techniques to minimize locking effects, such as shear locking or volumetric locking. Materials can be defined as isotropic or anisotropic, making the element versatile for composite modeling where fiber angles and ply orientations significantly affect the structural response.

The mathematical formulation includes strain-displacement relationships derived from shear deformation theory, equilibrium equations, and stiffness matrices. The stiffness matrix is typically expressed in terms of the ABD matrix, which combines in-plane and bending stiffness contributions for multilayered laminates. For a laminate with multiple layers, the total thickness is computed as the sum of individual layer thicknesses, and the ABD matrix incorporates the material properties and fiber orientations of all layers. This ensures an accurate representation of the composite's mechanical behavior under various loading conditions.

The First-Order Shear Deformation Theory (FSDT), also known as the Mindlin-Reissner plate theory, is a widely used approach for analyzing the behavior of laminated composite plates, particularly when transverse shear deformation effects are significant. It is especially suitable for thick plates, where classical plate theory (CPT) may be inaccurate due to its neglect of shear deformation. FSDT assumes that a straight line normal to the mid-surface before deformation remains straight but not necessarily normal after deformation, accounting for shear deformation. This leads to a displacement field expressed as:

$$\begin{aligned} u(x, y, z) &= u_0(x, y) + z\theta_x(x, y) \\ v(x, y, z) &= v_0(x, y) + z\theta_y(x, y) \\ w(x, y, z) &= w_0(x, y) \end{aligned} \quad (1)$$

where u_0, v_0, w_0 are Mid-surface displacements. Also, $\theta_x(x, y)$ and $\theta_y(x, y)$ Rotations of the normal about the y and x axes. So, according to the introduced displacement, the linear strain components are expressed as:

$$\varepsilon_{xx} = \frac{\partial}{\partial x} u_0(x, y) + \frac{\partial}{\partial x} \theta_x(x, y) \quad (2)$$

$$\varepsilon_{yy} = \frac{\partial}{\partial y} v_0(x, y) + \frac{\partial}{\partial y} \theta_y(x, y) \quad (3)$$

$$\begin{aligned} \varepsilon_{xy} &= \frac{\partial}{\partial y} u_0(x, y) + \frac{\partial}{\partial x} v_0(x, y) \dots \\ &+ z \left(\frac{\partial}{\partial y} \theta_x(x, y) + \frac{\partial}{\partial x} \theta_y(x, y) \right) \end{aligned} \quad (4)$$

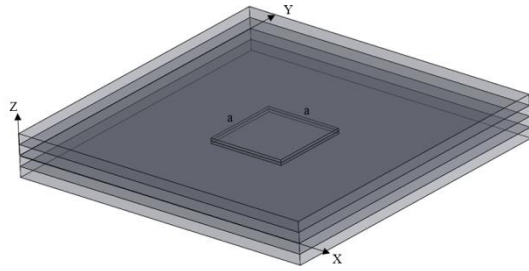


Fig. 1. Schematic view of considered laminated plate with delamination

Generally, the definition of the interaction behavior of adjacent layers in the delamination region is the effective parameter that determines the dynamic characterization of the plate. The actual status of delamination is simulated using extremely thin empty space to avoid modeling complexities. This empty space is inserted between the upper and lower sub-laminates within the delaminated region. The thickness of

empty space is specified as 5 μm in this study. The considered thickness avoids the contact interaction of the elements in the delaminated regions. Based on the mesh study of the model, 3600 elements (60 \times 60) were used to discretize the models. Also, only one element was utilized through the thickness according to the layering phenomena and integration point of the specified element. As shown in Fig.3, the number of elements was distributed along the sides of the model in such a way that the number of elements in the delaminated zone is a function of its area. This method allows for comparing the results of different models.

Calculating the stiffness matrix is the most important step in the finite element analysis of a laminated plate containing delamination zones. The presence of delamination can cause a significant reduction in stiffness and strength of the laminates. Obviously, to investigate the effect of delamination in natural frequencies, finite element modeling should be done in such a way that the separation of layers in the delaminated region has an effect on the final stiffness matrix of the structure. Based on the modal analysis, inter-layer failure behavior will not be considered. So, by avoiding methods such as cohesive zone modeling, the delamination is modeled as an empty space between the layers as stated earlier.

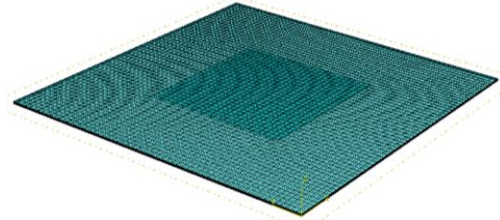


Fig. 2. Meshing of the laminated plate with 20% delaminated region

As shown in Fig. 2, the modeled empty space can be assumed as an inter-layer element with null mechanical properties. Thus, the definition of the element stiffness matrix for the delaminated area can be presented as follows:

$$K^e = \begin{bmatrix} B_1 D_{M1} B_1 & B_1 D_{M1} B_2 & B_1 D_{M1} B_3 & 0 & 0 & 0 \\ B_2 D_{M1} B_1 & B_2 D_{M1} B_2 & B_2 D_{M1} B_3 & 0 & 0 & 0 \\ B_3 D_{M1} B_1 & B_3 D_{M1} B_2 & B_3 D_{M1} B_3 + B_{3Int} D_{Int} B_{3Int} & B_{3Int} D_{Int} B_{4Int} & 0 & 0 \\ & & B_{4Int} D_{Int} B_{3Int} & B_{4Int} D_{Int} B_{4Int} + B_4 D_{M2} B_4 & B_4 D_{M2} B_5 & B_4 D_{M2} B_6 \\ & & & B_5 D_{M2} B_4 & B_5 D_{M2} B_5 & B_5 D_{M2} B_6 \\ & & & B_6 D_{M2} B_4 & B_6 D_{M2} B_5 & B_6 D_{M2} B_6 \end{bmatrix} \quad (5)$$

in this equation, B is the matrix of shape function derivatives for the M1 and M2 layers and interface space. Also, D represents the stiffness matrix of the layers. The superscripts of *Int* denote the interface space. The presented

element matrix is a typical laminate containing two layers connecting with a specified interface space (see Fig. 3). Based on the mentioned above, an empty space can be assumed as an inter-layer element with null mechanical properties. So, D_{Int}

relates to the interface properties of the layers which are assumed null for elements located in the delamination region.

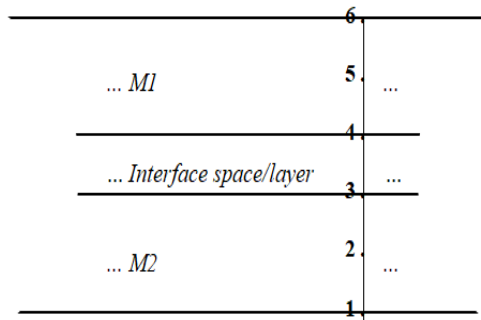


Fig. 3. Implementing of interface space between layers

3. Result and Discussion

In this study, the considered laminated plate is a square four-layer plate with various stacking sequences of layers. A T300 carbon-epoxy composite plate, with dimensions 300×300 mm² and 2 mm (4×0.5 mm) thickness is considered. The results based on the ABAQUS solution are stated here for simply supported boundary conditions. In the following, the effect of the stacking sequence of the layers, delaminated area, the size, number, and different arrangements of delaminated regions are analyzed on the natural frequency of the composite laminated plates. Before the presentation of the numerical results, verification of the presented finite element models is needed.

3.1. Validation

The proposed model herein proposed needs to be validated. To this aim, the vibrating behavior of a laminated plate with a specified delaminated region is considered according to the literature [10]. The results are successfully compared to predictions from the literature. In this validation, the laminated plate is made of composite material with the properties presented in Table 1. According to the mentioned literature, the delaminated region is placed in the middle of the laminate at the interface of mid-layers and its area is 0.125 × 0.125 m².

Table 1. Material properties considered for validation

E_1	E_2	G_{12}	$\nu_{12} = \nu_{13}$	ν_{23}	ρ
GPa			Kg/m ³		
132	5.3	2.79	0.291	0.3	1446.20

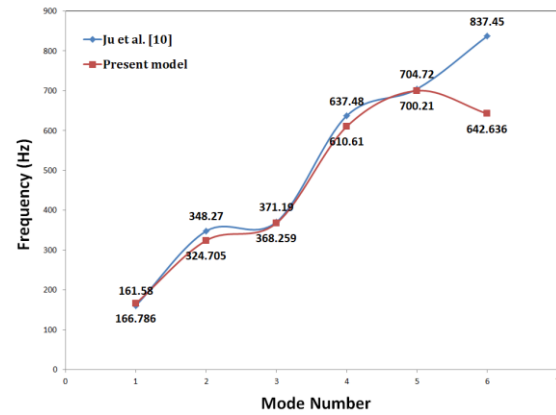


Fig. 4. Comparison of the natural frequencies of the literature [10] and obtained from the present model

Figure 4 compares the natural frequencies of the designed model with the results from the literature. As expected, there is some difference between the present results and those given mentioned reference. This could be due to the difference between the element properties and the theories used in the present study and the mentioned literature.

3.2. Stacking Sequence Effect

Natural frequencies of the laminated plates with different sizes of delaminations and different stacking sequences are presented in this section. In this study, the variation of the natural frequencies as a function of the delaminated area ratio, A_d , for the seven first modes is analyzed, where

$$A_d = \frac{\text{delamination area}}{\text{plate area}} \times 100 \quad (6)$$

The material properties and stacking sequences of the considered samples are presented in Table 2. In this study, the plates are composed of four layers made of unidirectional fabric fibers. Four layers represent the minimum number of layers for a multilayered plate, allowing for the investigation of various layup configurations. Increasing the number of layers will undoubtedly reduce the influence of the layup arrangement and fiber angles on the results.

In these samples, the delaminated region is placed in the middle of the plate and interface of layers 2 and 3 of the laminate. Also, the delaminated area ratio, A_d is considered between 10 to 60% for each laminate.

According to the plots shown in Figs. 5 to 7, the variation trend of natural frequencies of the considered models are function of the stacking sequences of the layers for each size of delaminated area.

As shown in Fig. 5, the numerical results of the symmetric laminate indicate that the variation trends of natural frequencies are different for each delaminated area ratio and vibration mode. According to the results, the increase in delaminated area ratio has a reducer effect on natural frequency for all mode shapes. This phenomenon can help to evaluate the size of the delaminated region accurately using specified mode shape and natural frequency for the symmetric laminates.

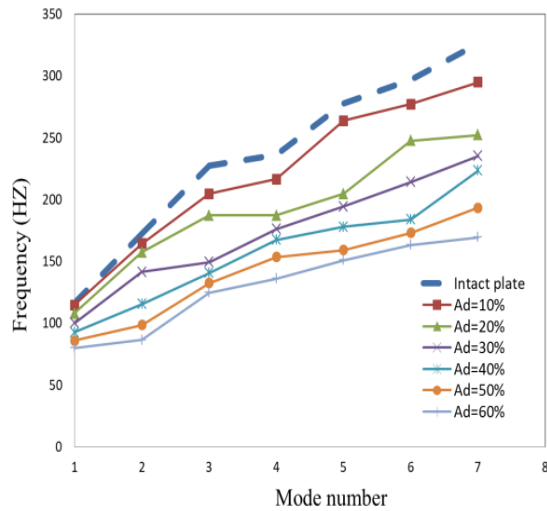


Fig. 5. Natural frequencies of the symmetric laminates according to the delaminated area ratio (A_d)

Based on Fig. 6, the results of the antisymmetric laminate showed that the reducer effect of delamination size is not the same for each mode shape. In fact, there is no specific trend based on the delaminated area ratio before the sixth mode. Therefore, it can be concluded that the higher mode shapes (here sixth and seventh modes) can be used to predict delamination characteristics for antisymmetric laminates.

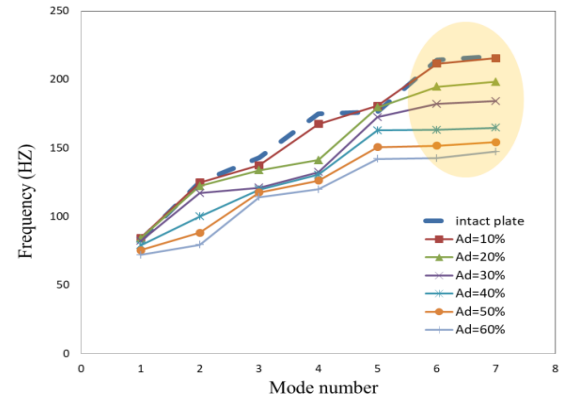


Fig. 6. Natural frequencies of the antisymmetric laminates according to the delaminated area ratio (A_d)

As presented in Fig. 7, the trends of the results are similar to the antisymmetric laminate for cross-ply laminate. The numerical results stated that the reducer effect of delamination size was achieved only for mode seven in the first seven vibration modes. In general, the numerical results of the symmetric and anti-symmetric laminate indicated that decreasing the natural frequency is not necessarily a function of increasing the delamination area in lower mode shapes. The numerical results indicate that from mode 6 onwards, the outcomes reach a certain regularity.

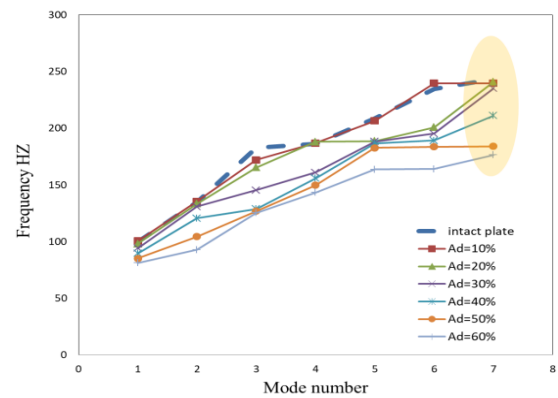


Fig. 7. Natural frequencies of the cross-ply laminates according to the delaminated area ratio (A_d)

Table 2. The characteristics of the constituent material of the considered laminated plates

Laminated plate	Symmetric	Antisymmetric			Cross ply
	$[30/60]_s$	$[30/60/-60/-30]$			$[0/90]_2$
$E_1 = E_2$ (Pa)	E_3 (Pa)	G_{12} (Pa)	$\nu_{12} = \nu_{13}$	ν_{23}	ρ (Kg/m^3)
70	10	10	0.1	0.2	1800

3.3. Effect of Delaminated Region Arrangements

Generally, specification of the region containing several defects and analysis of the effective parameters of this region is an important topic in health monitoring of the laminated plates and shells. So, the effect of the number and arrangement of delaminated regions are the other parameters that are investigated in this study. The ratio of the area containing all delaminated regions (called high-risk zone) to the total area of the laminated plate is the parameter that is used to analyze the number and arrangement of the delaminated regions. As shown in Fig. 8, the high-risk zone ratio, A'_d , is defined as follows:

$$A'_d = \frac{\text{area of high risk zone}}{\text{plate area}} \times 100 \quad (7)$$

Briefly, the obtained natural frequencies of the many considered models indicated that the effect of several delaminated regions is different from their sum in one location. In this study, the effect of some delaminated regions in different locations is analyzed on the natural frequencies of the laminated plates. The comparison of the achieved results with the natural frequencies of the intact laminated plate and the main delaminated plate (a laminate that contains a delaminated region with the same size as the sum of all delaminated regions) is the aim of the following sections.

3.3.1. Two Delaminated Regions

According to Fig. 8, a delaminated region with a 20% delaminated area ratio, is divided into two equal delaminated regions in the modeling of the plate. The delaminated regions are located in four positions at different distances from each other. The analysis of these models with specifications presented in Table 2 showed different results based on the stacking sequences.

As shown in Fig. 9, the numerical results of the symmetric laminate with two delaminated regions stated that the natural frequencies of all modes are between the frequency of the intact laminate and the main delaminated plate. Therefore, if the natural frequency of the delaminated plate (in comparison with the intact plate) is considered as a criterion to determine its health level, it can be concluded that the destructive effect of two delaminated regions with different distances is less than one delaminated region with an area equal to the sum of those areas.

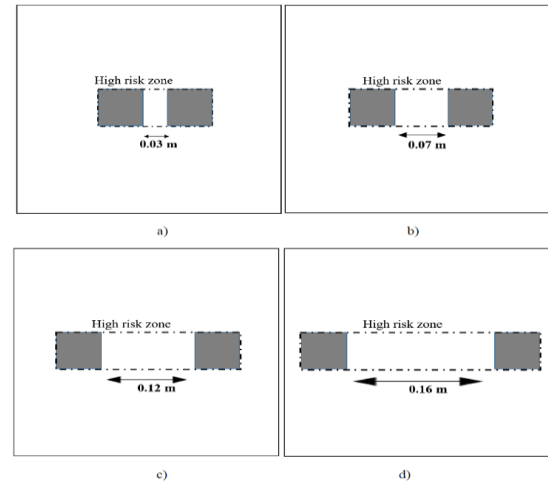


Fig. 8. The view of the four locations of the two delaminated regions

In this study, the percentage of the frequency shift of the samples is defined as

$$\text{frequency shift}(\%) = \frac{f_{sdr} - f_{mdp}}{f_{sdr}} \times 100 \quad (8)$$

where f_{sdr} is the natural frequency of the laminated plate with several delaminated regions and f_{mdp} is the natural frequency of the main delaminated plate. The achieved frequency shifts of all samples with two delaminated regions (see Fig. 8) and the main delaminated plate are presented in Fig. 10 for the symmetric stacking sequence. As shown in this figure, the maximum frequency shift is obtained at 26.37% for the main delaminated plate in mode 5. However, the highest frequency shifts are obtained in modes 3 for samples (c) and (d) and 6 for samples (a) and (b). So according to the results, the third, fifth, and sixth modes play the most important role in investigating the delamination effect.

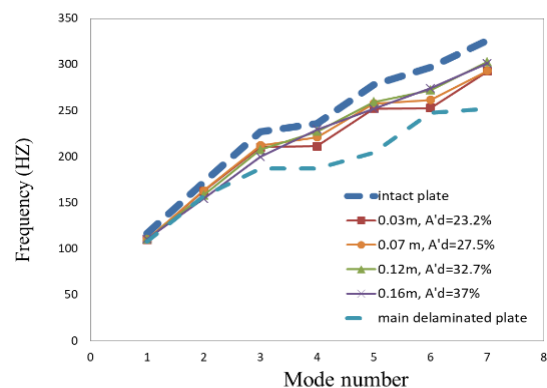


Fig. 9. Variation of natural frequencies of the symmetric laminates (2 delaminated regions)

Also, the resulting natural frequencies indicated that the variation trends of the samples with two delaminated regions according to the distance of these regions are not the same for all mode shapes in symmetric laminated plates.

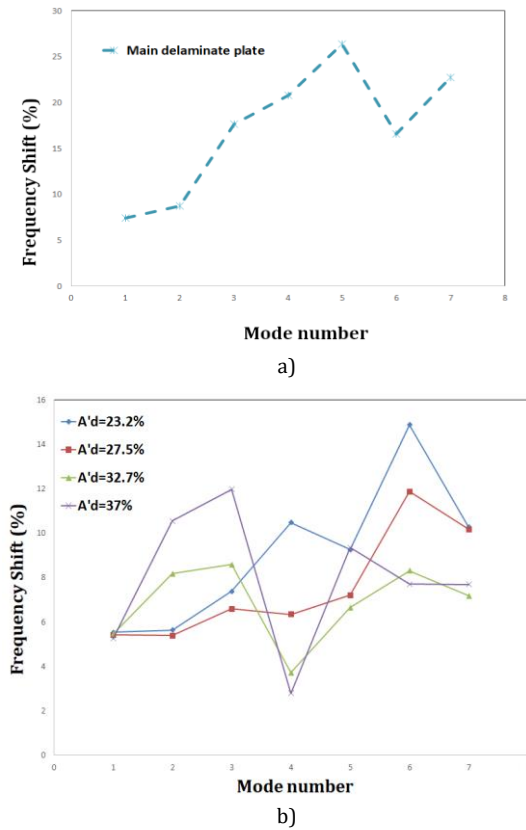


Fig. 10. The frequency shift of the symmetric samples (2 delaminated regions)

According to Fig. 11, the obtained results of the anti-symmetric laminates show some disorders. According to the results, there are only modes 3, 4, and 6 their frequencies are between the intact plate and the main delaminated plate. Moreover, the results of the anti-symmetric laminated plate revealed that the maximum frequency shift is obtained at 19.37% for the main delaminated plate in mode 4. Also, the maximum frequency shifts are achieved in modes 3 and 6 for all samples with two delaminated regions. So, these modes are important for anti-symmetric laminates to specify delamination properties.

The results of the cross-ply laminate which are shown in Fig. 13, indicated some disorders similar to anti-symmetric laminate. There are not any modes that its all frequencies between the intact plate and the main delaminated plate.

Also based on Fig. 14, there are ascending trends in natural frequencies according to the size of the high-risk zone for modes 1 and 3. As indicated in Fig. 14, the maximum frequency shift is achieved by 14.45% for the main delaminated plate in mode 6. In addition, modes 3 and 5 have the maximum frequency shift for all samples with two delaminated regions. These mode numbers are useful for analyzing the delamination effects in cross-ply laminated plates.

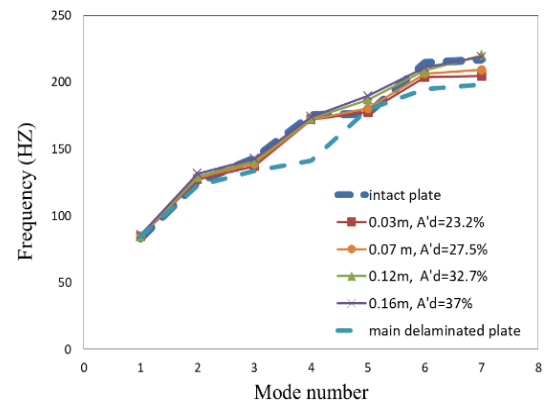


Fig. 11. Variation of natural frequencies of the anti-symmetric laminates (2 delaminated regions)

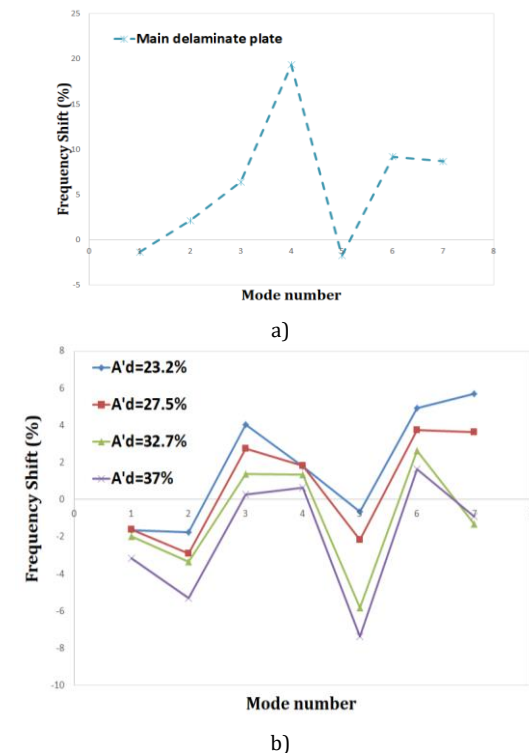


Fig. 12. The frequency shift of the anti-symmetric samples (2 delaminated regions)

Based on Fig. 8, The mode shapes of the considered samples, with maximum frequency shift, are shown for two high-risk zone ratios. $A'd = 23.2\%$ and $A'd = 37\%$ in Fig. 15. It can be seen that the mode shapes are affected by the location of delaminations. This phenomenon can be useful in tracking the delamination regions and their number and arrangement.

For symmetric laminated plates that contain two delaminated regions, the maximum frequency shift is obtained at 14.89 % in mode 6, and for the case where the high-risk zone ratio is 27.2%. This parameter is obtained at 5.69% in mode 7 and with a high-risk zone ratio of 27.2% for anti-symmetric laminated plate 7.11% in mode 5 and 27.5% high-risk zone ratio for cross-ply laminated plate.

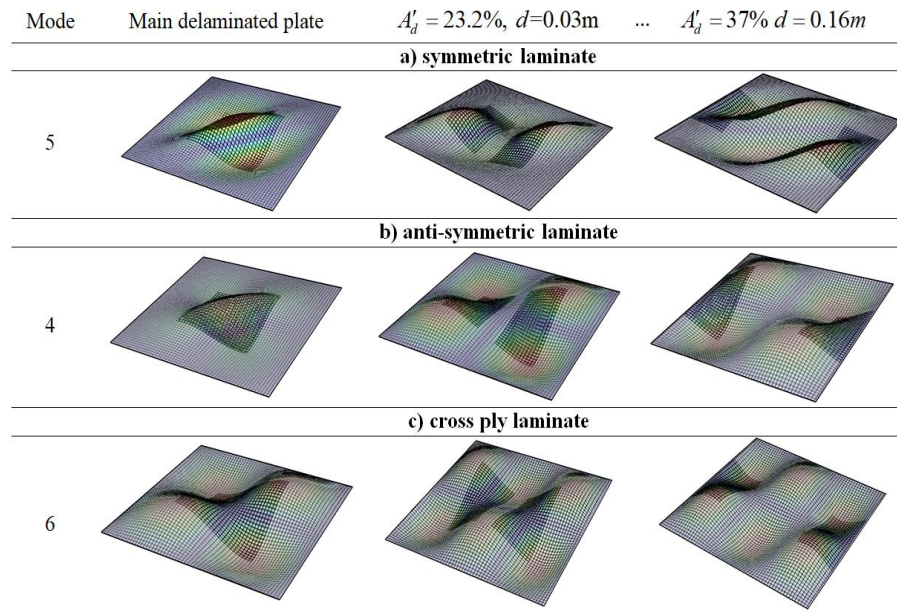


Fig. 15. The mode shapes of the main delaminated plates and the plates with two delaminated regions which have the maximum frequency shift

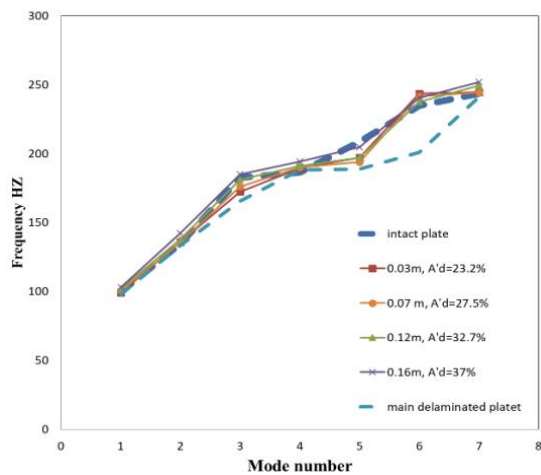


Fig. 13. Variation of natural frequencies of the cross-ply laminate according to the mode number (2 delaminated regions)

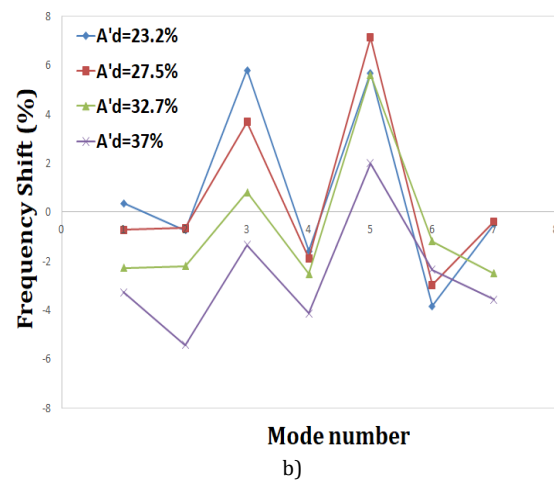
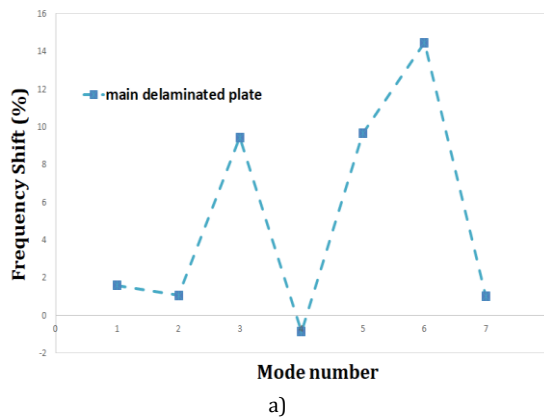


Fig. 14. The frequency shift of the anti-symmetric samples with two delaminated regions according to the mode number (2 delaminated regions)



3.3.2. Four delaminated regions

The analysis of the high-risk zones containing four delaminated regions is another topic that is investigated here (see Fig. 16). Symmetric, anti-symmetric, and cross-ply are the stacking sequences that were considered before. The numerical results are shown in Figs. 17-19.

The obtained results of symmetric laminates indicate that the natural frequencies of all modes are between the frequency of the intact laminate and the main delaminated plate for all considered high-risk zone ratios.

However, the results of anti-symmetric and cross-ply laminates do not show this phenomenon. However, the resulting natural frequencies of all samples with four delaminated regions are close to the intact laminate frequencies. It could be due to the smallness of the delamination regions and the ineffectiveness of them. Therefore, it can be concluded that the effect of the size of the delamination regions on the dynamic characterization of the laminated plate is much greater than their number.

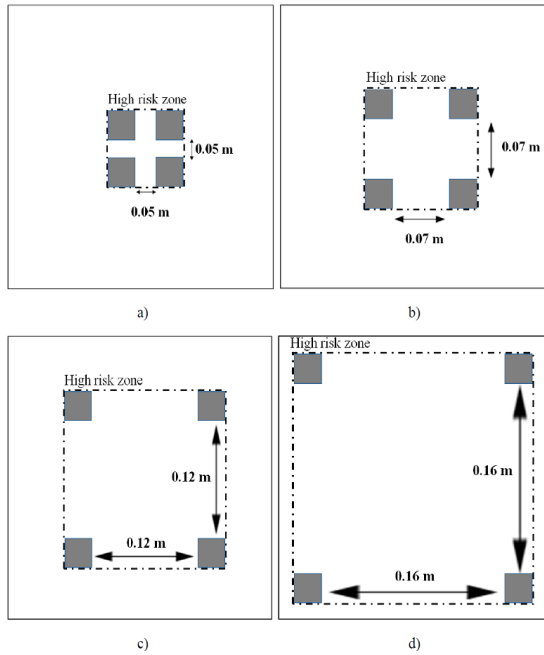


Fig. 16. The view of the four locations of the four delaminated regions

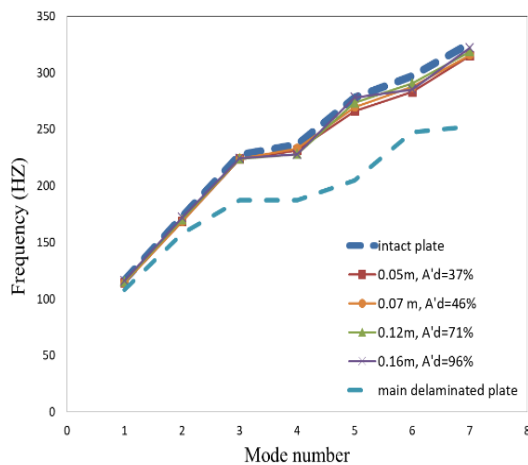


Fig. 17. Variation of natural frequencies of the symmetric laminate according to the mode number (4 delaminated regions)

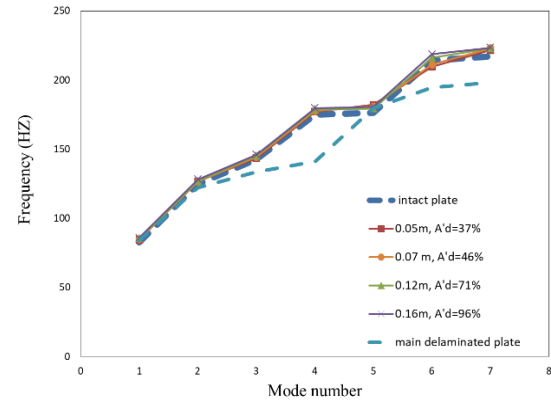


Fig. 18. Variation of natural frequencies of the anti-symmetric laminate according to the mode number (4 delaminated regions)

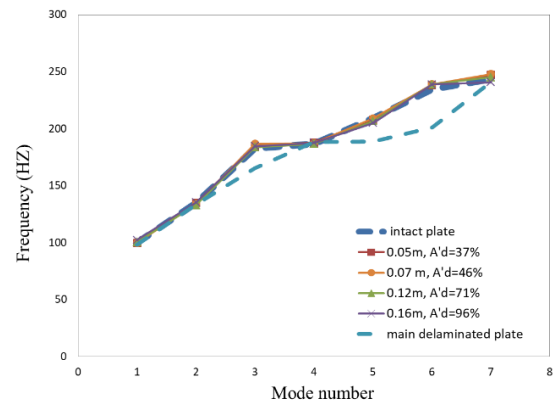


Fig. 19. Variation of natural frequencies of the cross-ply laminate according to the mode number (4 delaminated regions)

Frequency shifts of all samples with four delaminated regions (see Fig. 16) are presented in Figs. 20-22 for the symmetric, anti-symmetric, and cross-ply stacking sequences. As shown in Fig. 20, the maximum frequency shifts are obtained in modes 4 for samples (c) and (d) and 6 for samples (a) and (b). So, considering the results of the samples with four delaminated regions, the fourth and sixth frequencies of the symmetric laminated plate show the maximum effect of the arrangement of delaminated regions.

According to Fig. 21, for anti-symmetric laminates, the maximum frequency shifts are gained in modes 4 and 6. Here too, the results indicate that mode 6 is the effective vibration mode number.

For cross-ply laminates, the value of maximum frequency shifts resulted in modes 5 and 6 (see Fig. 22). This mode number has an important role in detecting delamination similar to the samples with two delaminated regions.

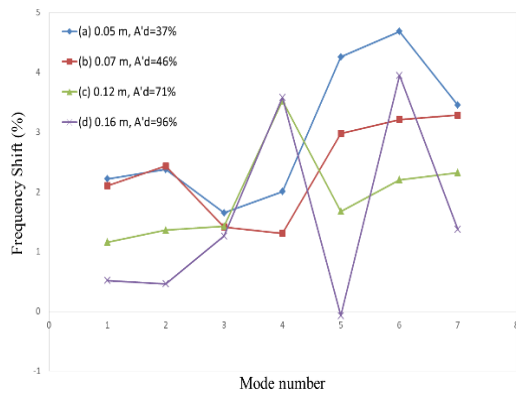


Fig. 20. The frequency shift of the symmetric samples with four delaminated regions according to the mode number (4 delaminated regions)

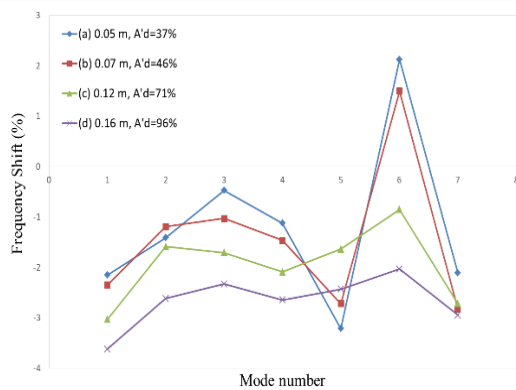


Fig. 21. The frequency shift of the anti-symmetric samples with four delaminated regions according to the mode number (4 delaminated regions)

Generally, the achieved natural frequencies of the samples indicate that the vibrational modes 4 to 6 are the effective modes for the laminated plate with one delaminated region. However, the vibrational modes 5 to 7 are the effective modes

for the assessment of the delamination effect of the laminates with several delamination regions.

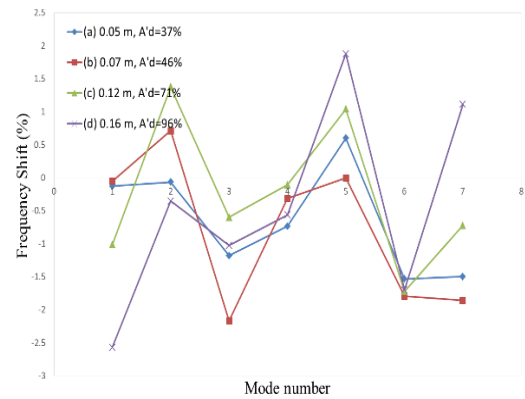


Fig. 22. The frequency shift of the cross-ply samples with two delaminated regions according to the mode number (4 delaminated regions)

According to Fig. 23, the mode shapes of the laminated plate with four delaminated regions are different from their main delaminated plate. However, the change in distance of the delaminated regions from each other does not affect the mode shapes of the laminated plates. It seems that the smallness of the delaminated regions (in these samples) leads to the lack of effect of their arrangements on the mode shapes.

Finally, the numerical results indicate that for laminated plates which contain four delaminated regions, the maximum frequency shift is obtained at 4.68 % in mode 6 and 37% high-risk zone ratio for symmetric stacking sequence, 2.12 % in mode 6 and 37% high-risk zone ratio for anti-symmetric stacking sequence and finally 2.16 % in mode 3 and 46% high-risk zone ratio for cross-ply stacking sequence.

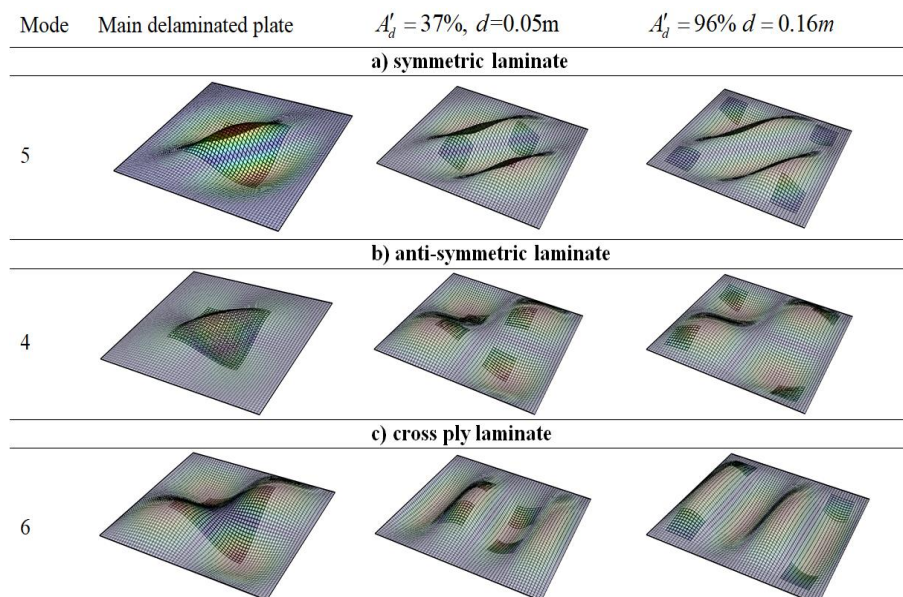


Fig. 23. The mode shapes of the main delaminated plates and the plates with four delaminated regions which have the maximum frequency shift

4. Conclusions

Modal analysis has been conducted on the four-layer square laminated plate with several delaminated regions with different numbers and arrangements. Extended parametric results were presented to investigate the influence intensity of the geometric parameters of the delaminated regions such as size, distances of the regions, and arrangements on the vibration response of the considered laminated plates. In this study, an attempt has been made to analyze all common cases of layer stacking sequences. Additionally, efforts were made to quantitatively investigate and compare the effect of the distribution of delaminated points.

- Accordingly, the analysis was implemented based on the FSDT in the framework of the FEM using ABAQUS solver. The main numerical results are expressed in a few words:
- The mode numbers that present maximum frequency shift are the same for the samples with two and four delaminated regions. This phenomenon was not seen in the frequency shifts of the samples compared to the intact laminates.
- Increasing of delamination size has a reducer effect on the natural frequency for all mode shapes in symmetric laminated plates. But in return, increasing of delamination size causes to increase in the natural frequency in some mode shapes for anti-symmetric and cross-ply laminated plates.
- Based on modal analysis of geometrical parameters of the delaminated regions, the size of these areas is more effective than their numbers and arrangements.
- According to the achieved results, high vibrational modes (modes 4 and up) can be useful for the assessment of the health of a laminated plate.
- According to the mentioned results, by detecting multiple delaminated regions in a structure, a decision can be made based on the destructive effect of a delaminated region with the total area of these zones. This method is a conservative solution.

Funding Statement

This research did not receive any specific grant from funding agencies in the public, commercial, or not-for-profit sectors.

Conflicts of Interest

The author declares that there is no conflict of interest regarding the publication of this article.

References

- [1] Senthil, K., Arockiarajan, A., Palaninathan, R., Santhosh, B., & Usha, K. M., 2013. Defects in composite structures: Its effects and prediction methods – A comprehensive review. *Composite Structures*, 106, pp. 139–149.
- [2] Krueger, R., & O'Brien, T. K., 2001. A shell/3D modeling technique for the analysis of delaminated composite laminates. *Composites Part A: Applied Science and Manufacturing*, 32(1), pp. 25–44. [https://doi.org/10.1016/S1359-835X\(00\)00133-0](https://doi.org/10.1016/S1359-835X(00)00133-0)
- [3] Caron, J.F., Diaz, A.D., Carreira, R. P., Chabot, A., & Ehrlacher, A., 2006. Multi-particle modeling for the prediction of delamination in multi-layered materials. *Composites Science and Technology*, 66(6) pp. 755-765.
- [4] Saeedi, N., Sab, K., & Caron, J. F., 2012. Delaminated multilayered plates under uniaxial extension. Part II: Efficient layerwise mesh strategy for the prediction of delamination onset. *International Journal of Solids and Structures*, 49(26), pp.3727–3740. <https://doi.org/10.1016/j.IJSTR.2012.08.003>
- [5] Mallikarjuna, & Kant, T., 1988. Dynamics of laminated composite plates with a higher order theory and finite element discretization. *Journal of Sound and Vibration*, 126(3), pp. 463–475.
- [6] Zou, Y., Tong, L., & Steven, G. P., 2000. Vibration-Based Model-Dependent Damage (Delamination) Identification and Health Monitoring for Composite Structures — A Review. *Journal of Sound and Vibration*, 230(2), pp. 357–378.
- [7] Ye, N., Su, C., & Yang, Y., 2021. Free and Forced Vibration Analysis in Abaqus Based on the Polygonal Scaled Boundary Finite Element Method. *Advances in Civil Engineering*, 2021(1), p.7664870.
- [8] Della, C. N., & Shu, D., 2007. Vibration of Delaminated Composite Laminates: A Review. *Applied Mechanics Reviews*, 60(1), pp. 1–20.
- [9] Barbero, E. J., & Reddy, J. N., 1991. Modeling of delamination in composite laminates using a layer-wise plate theory. *International Journal of Solids and Structures*, 28(3), pp. 373-388.
- [10] Moorthy CMD, Reddy JN., 1998. Modelling of laminates using a layerwise element with

- enhanced strains. *Int. J. Numer. Meth. Eng.*, 43(4), pp. 755-779.
- [11] Ju, F., Lee, H.P., & Lee, K.H., 1995. Finite element analysis of free vibration of delaminated composite plates. *Composites Engineering*, 5(2), pp. 195-209.
- [12] Kim, H.S., Chattopadhyay, A., and Ghoshal, A., 2003. Characterization of delamination effect on composite laminates using a new generalized layerwise approach. *Computers and Structures*, 81(15), pp. 1555-1566.
- [13] Hu, N., Fukunaga, H., Kameyama, M., Aramaki, Y., and Chang, F. K., 2002. Vibration analysis of delaminated composite beams and plates using a higher-order finite element. *International Journal of Mechanical Sciences*, 44(7), pp. 1479-1503.
- [14] Yam, L.H., Wei, Z., Cheng, L., and Wong, W.O., 2004. Numerical analysis of multi-layer composite plates with internal delamination. *Computers and Structures*, 82(7-8), pp. 627-637.
<https://doi.org/10.1016/j.compstruc.2003.12.003>
- [15] Kuo, S.Y., 2011. Effect of delamination on natural frequencies of rectangular laminates. *Journal of Aeronautics, Astronautics and Aviation*, 43(3), pp. 209-218.
- [16] Hammami, M., El Mahi, A., Karra, C., & Haddar, M., 2016. Experimental analysis of the linear and nonlinear behaviour of composites with delaminations. *Applied Acoustics*, 108, pp. 31-39.
<https://doi.org/10.1016/j.apacoust.2015.10.026>
- [17] Khazaee, M., Nobari, A.S., & Aliabadi, M. H. F., 2018. Experimental investigation of delamination effects on modal damping of a CFRP laminate, using a statistical rationalization approach. In *Vibration-Based Techniques for Damage Detection and Localization in Engineering Structures*, (pp. 75-103).
https://doi.org/10.1142/9781786344977_0003
- [18] He, Y., Xiao, Y., & Su, Z., 2019. Effects of surface contact on the dynamic responses of delaminated composite plates. *Composite Structures*, 229, p. 111378.
- [19] Yang, C., Huang, B., Guo, Y., & Wang, J., 2021. Characterization of delamination effects on free vibration and impact response of composite plates resting on visco-Pasternak foundations. *International Journal of Mechanical Sciences*, 212, p.106833.
- [20] Kumar, S.K., Harursampath, D., Carrera, E., Cinefra, M., & Valvano, S., 2018. Modal analysis of delaminated plates and shells using Carrera Unified Formulation-MITC9 shell element. *Mechanics of Advanced Materials and Structures*, 25(8), pp. 681-697.
- [21] Dey, S., & Karmakar, A., 2012. Effect of location of delamination on free vibration of cross-ply conical shells. *Shock and Vibration*, 19(4), pp. 679-692.
- [22] De Menezes, V. G. S., Souza, G. S. C., Vandepitte, D., Tita, V., & de Medeiros, R., 2021. Defect and damage detection in filament wound carbon composite cylinders: A new numerical-experimental methodology based on vibrational analyses. *Composite Structures*, 276, p.114548.
- [23] He, M., Ramakrishnan, K. R., Wang, Y., Zhang, Z., & Fu, J., 2022. A combined global-local approach for delamination assessment of composites using vibrational frequencies and FBGs. *Mechanical Systems and Signal Processing*, 167, p.108577.
- [24] Joy, E. J., Biju, N., & Menon, A. S., 2019. Delamination detection in composite laminates using ensemble of surrogates. *Materials Today: Proceedings*, 46, pp. 9597-9603.
- [25] Lim, D. K., Mustapha, K. B., & Pagwiwoko, C. P., 2021. Delamination detection in composite plates using random forests. *Composite Structures*, 278, p.114676.
- [26] Tong, H., Pan, J., Singh, H. K., Luo, W., Zhang, Z., & Hui, D., 2021. Delamination detection in composite laminates using improved surrogate-assisted optimization. *Composite Structures*, 277, p.114622.
- [27] Maurya, M., Sadarang, J., Panigrahi, I., & Dash, D., 2022. Detection of delamination in carbon fibre reinforced composite using vibration analysis and artificial neural network. *Materials Today: Proceedings*, 49, pp. 517-522.
- [28] Zhang, Z., He, M., Liu, A., Singh, H.K., Ramakrishnan, K.R., Hui, D., Shankar, K., & Morozov, E.v., 2018. Vibration-based assessment of delaminations in FRP composite plates. *Composites Part B: Engineering*, 144, pp. 254-266.
- [29] Sha, G., Cao, M., Radziński, M., & Ostachowicz, W., 2019. Delamination-induced relative natural frequency change curve and its use for delamination localization in laminated composite beams. *Composite Structures*, 230, p.111501.

- [30] Gomes GF, Mend'ez YAD, da Silva Lopes Alexandrino P, da Cunha SS, Ancelotti AC., 2018. The use of intelligent computational tools for damage detection and identification with an emphasis on composites—a review. *Compos Struct*, 196, pp. 44–54.
- [31] Alkayem NF, Cao M, Zhang Y, Bayat M, Su Z., 2018. Structural damage detection using finite element model updating with evolutionary algorithms: a survey. *Neural Comput Appl*, 30(2), pp. 389–411.
- [32] Gordan M, Razak HA, Ismail Z, Ghaedi K., 2017. Recent developments in damage identification of structures using data mining. *Latin American Journal of Solids and Structures*, 14(13), pp. 2373–2401.
- [33] Nag A, Mahapatra DR, Gopalakrishnan S., 2002. Identification of delamination in composite beams using spectral estimation and a genetic algorithm. *Smart Mater Struct*, 11(6), pp. 899–908.
- [34] Krawczuk M, Ostachowicz W., 2002. Identification of delamination in composite beams by genetic algorithm. *Science and Engineering of Composite Materials*; 10, pp. 147–56.
- [35] Xia, S., Wang, Z., Lin, C., & Xu, H., 2024. Vibration Analysis of Laminated Composite Plates with Delamination Damage. In S. Fu (Ed.), *Asia-Pacific International Symposium on Aerospace Technology (APISAT 2023) Proceedings* (pp. 833–842). Springer. 3998-1_69
- [36] Krawczuk, M., Ostachowicz, W., & Żak, A., 2023. Natural vibration frequencies of delaminated composite beams. *Computer Assisted Methods in Engineering and Science*, 3(3), pp. 233–243.